Solar Energy Materials and Solar Cells 27 (1992) 189–216
North-Holland

Solar Energy Materials and Solar Cells

Spectral effects on PV-device rating

S. Nann [a] and K. Emery [b]

[a] *Centre for Solar Energy and Hydrogen Research, Hessbruehlstrasse 61, W-7000 Stuttgart 80, Germany*
[b] *National Renewable Energy Laboratory, 1617 Cole Boulevard, Golden, CO 80401, USA*

Received 22 May 1991; in revised form 24 October 1991

A recently developed spectral model "SEDES2" is applied to study the effect of variations in solar spectral irradiance on the efficiency of seven particular solar cells. As a new feature, SEDES2 calculates hourly solar spectral irradiance for clear and cloudy skies from readily available site-specific meteorological data. Based on these hourly spectra, monthly and yearly efficiencies for the solar cells are derived. As a key result the efficiencies of amorphous silicon cells differ by 10% between winter and summer months because of spectral effects only. A second intention of this study is to analyse the sensitivity of power and energy rating methods to spectral irradiance but also to total irradiance and cell temperature. As an outcome, a multi-value energy rating scheme applying the concept of "critical operation periods" is proposed.

1. Introduction

For a solar device operating in the terrestrial environment the efficiency will depend on its operating cell temperature, and the total and spectral irradiance. Working in the field of PV-system simulation, we are interested in predicting the efficiency a given PV-technology will obtain at a given site and time. The site should be characterized by a few easily available climatological parameters. This has not been possible yet for arbitrary sites and seasons because one could not simulate the solar spectral irradiance for partly cloudy and overcast sky conditions. Under cloudy skies PV-systems deliver only a fraction of their annual energy. Nevertheless, an investigation including partly cloudy and overcast skies is important to answer the following questions:

(1) What are the quantitative sensitivities of device performance to spectral variations caused by cloud, water vapor, aerosols, air mass, etc.? And how are these sensitivities related to the total integrated power produced by PV-devices?

(2) What is the efficiency of a PV-system during the period with the lowest insolation (winter), when clouds may cover the sun for several weeks? This becomes important for the design of storage size of a remote system.

Correspondence to: K. Emery, National Renewable Energy Laboratory, 1617 Cole Boulevard, Golden, CO 80401, USA.

(3) What does a representative spectrum look like for climates where the sunlight is attenuated by clouds for 50% or more of the daylight period?

(4) What spectrum (or spectra) should be used to design a PV-device for optimum outdoor performance?

(5) How large is the error due to spectral effects if one determines the efficiency of a PV-system outdoors measuring only cell temperature, total irradiance, and DC-output, but not the spectrum?

(6) How big are the losses for multijunction devices when different photocurrent densities originating in the top and bottom cells cause mismatch losses because the device was optimized for clear sky conditions with the AM1.5 reference spectrum?

(7) Is the difference in efficiency of amorphous silicon modules between winter and summer caused by temperature effects (annealing) or spectral effect?

Therefore, the Center of Solar Energy and Hydrogen Research (ZSW) started in 1989 to measure the solar spectral irradiance every five minutes along with basic meteorological parameters. Two solar spectral data acquisition systems are operated. They are located near Stuttgart (Germany, 49°N 9°E), a region with about 1800 sunshine hours a year (40% of daylight hours). In a combined effort with the Solar Energy Research Institute (SERI) these data were analyzed to develop a semi-empirical model which uses three easily available meteorological parameters to estimate solar spectral irradiance under clear, partly cloudy and overcast skies [1]. This unique and new model called SEDES2 will briefly be described and applied to investigate spectral effects on PV-cell performance under clear and cloudy skies.

We combine this spectral parametrization with solar cell measurements of some important state-of-the-art devices performed at SERI's calibration lab. Our study includes a three-junction, two-terminal device made from amorphous silicon. It is of special interest to compare the performance of the three-junction with a one-junction device's performance, because it is still open whether spectral effects (current mismatch) prevent the three-junction device from outperforming the one-junction device in cloudy climates.

The present investigation contributes to a research area developing methods for "power rating" and "energy rating". Energy rating is more complex than power rating which is the common procedure to attribute a "name-plate rating" to a solar cell or module. The current standard power rating method consists of a single-value specification of efficiency. This efficiency is measured for non-concentrator terrestrial photovoltaic cells under standard reporting conditions (1000 W/m^2 insolation, 25°C cell temperature, AM1.5 global reference spectrum) [2]. Energy rating, on the other hand, is site and time specific with one or several values characterizing the energy output of a PV-technology for a given site and period.

It has been reported by field experiments that photovoltaic modules do not meet their name-plate power rating under actual operating conditions by 10% to 30% on an annual average [3,4]. This discrepancy is caused by the following effects [5]:

(1) Modules operate at cell temperatures ranging from the ambient temperature to temperatures which are about 40°C above the ambient temperature (non-concentrating).

(2) The incident irradiance varies between 0 and 1200 W/m^2 standard.

(3) In addition, there are changes in the relative spectral distribution which lead to higher or lower efficiencies compared to the efficiency under the AM1.5 reference spectrum.

(4) At high angles of incidence the incoming light is more reflected than at direct normal incidence indoors under the light of the solar simulator [6]. Additional transmission losses are caused by soiling.

(5) The name-plate rating itself is guaranteed by the manufacturers only within a certain range (module-to-module variability).

(6) Partly, the discrepancies are caused by module degradation.

(7) Maximum power point tracking is off by some percent in most cases.

In this report we analyze the first three effects.

With a few exceptions, all PV-modules have been overrated because the single-value specification of efficiency under standard reporting conditions is a more favorable specification than that measured outdoors under real conditions. This discrepancy, however, should occur between measurements and rating, but not between rating and customer. It is important that an agreement is reached within the PV-community (customers, manufacturers, system designers, and scientists) on how to rate solar modules and cells closer to their real performance. Discrepancies between instantaneous field measurements and module rating become especially important when the instantaneous measurement is part of a contractual agreement between the vendor and customer. This becomes even more important if new cell technologies will be applied. Compared to crystalline silicon cells, linearity in temperature and irradiance response is not valid for most of the thin film devices and the spectral sensitivity of the higher band gap devices like a-Si, CdTe, or GaAs is more pronounced.

As a contribution to this we investigated how the meteorological environment influences cell/module efficiency at a cloudy site (Stuttgart, Germany) over the period of three years and how spectral variations affect power and energy rating schemes. A customer oriented multivalue specification of cell/module efficiency for critical operation periods will be proposed. This set of efficiencies shows that the selection of a PV-technology should not only be driven by the price per Watt but also by the efficiency during critical operation periods depending on the application, time, and site. Indeed, it is mainly the energy the customer buys and not the power.

2. Approach

Consider a PV-device operating outdoors with the optical/electrical behaviour of the cells as measured in the lab indoors and the thermal behaviour of a module exposed to the actual weather. The operating mode is a fixed latitude-tilted

flat-plate (non-concentrator). Electrical losses due to cell and module connection (mismatch, resistance), other wiring losses, and optical losses due to reflection or soiling are not taken into account. The device is operated at the maximum power point. The weather is characterized by hourly sums of global and diffuse irradiance, hourly averages of ambient temperature, relative humidity, surface pressure, and wind speed.

2.1. Solar cell model and data

This investigation comprises typical production mono-crystalline silicon (mono-Si), state-of-the-art GaAs, thin film technologies including CdS/CdTe and CdS/$CuInSe_2$, and amorphous silicon (a-Si:H) devices. The a-Si:H material is represented with three different designs: a single junction cell, a multijunction a-Si:H/a-Si:H/a-SiGe:H two-terminal device, where the efficiency is raised by integrating a-Si:H with a-SiGe:H alloy cells, and a four-terminal stack consisting of a-Si:H on $CuInSe_2$ cells. The electrical characteristic of the solar cell is computed with the so-called "two-diode equation", a superposition of dark and illuminated characteristics:

$$J_{ph} = (q/hc)\int_{320}^{1400} \lambda E(\lambda) \mathrm{QE}(\lambda)\, \mathrm{d}\lambda, \tag{1}$$

$$J_{0i} = J_{00i} \exp(-\Delta E_i / kT_c), \tag{2}$$

$$J_{dark} = J_{01}[\exp(qV/n_1 kT_c) - 1] + J_{02}[\exp(qV/n_2 kT_c) - 1], \tag{3}$$

$$J_{out} = J_{ph} - J_{dark} - V/R_{sh}, \tag{4}$$

$$V_{out} = V - J_{out} R_s, \tag{5}$$

$$P = J_{out} V_{out}, \tag{6}$$

$$\eta = P_{max}/I, \tag{7}$$

$$I = \int_{300}^{4000} E(\lambda)\, \mathrm{d}(\lambda). \tag{8}$$

The above summarized equations are based on the following physical assumptions:

(1) The temperature dependence of the reverse saturation current J_{0i} of both diodes is given in eq. (2) with an activation energy ΔE_i and constant J_{00i} applying the Meyer–Neldel rule [7,8].

(2) The quantum efficiency QE(λ) is independent of voltage, light bias, and cell temperature T_c (eq. (1)).

(3) The output current J_{out} is calculated by a superposition of the photocurrent J_{ph} and the dark current J_{dark} corrected for the shunt resistance R_{sh}, but not for the series resistance R_s (eq. (4)). Thus, an explicit equation is obtained.

(4) The diode quality factors n_1 and n_2 represent recombination losses which add to J_{dark} (eq. (3)). They are constant.

(5) R_{sh} represents leakage losses across the junction and around the cell's edges. It is fixed.

(6) R_s represents bulk, contact, interconnection, cabling and wiring resistance. It is fixed.

This model is applied to calculate the maximum power P_{max} for each set of irradiance, spectrum and cell temperature values. We are aware of the fact that the superposition principle has only been verified within a few percent for silicon and GaAs cells [9] but not for thin-film devices; that R_s, R_{sh}, n_i, and QE(λ) are, in general, a function of total irradiance, temperature, and voltage [10–13]. All these aspects must be investigated elsewhere. For the time being, we choose a very straightforward approach:

(1) QE(λ) is measured very accurately by methods described in refs. [2,14] at $T_c = 25°C$ and $I = 1000\ W/m^2$ (values see fig. 1).

(2) Initial guesses for R_s, R_{sh}, n_i, J_{00i}, and ΔE_i are obtained from the measured J–V characteristics.

(3) Eqs. (1)–(6) together with a search algorithm are applied to calculate the open-circuit voltage V_{oc}, the fill factor FF, and the maximum power P_{max}. These calculations are compared with V_{oc}, FF and P_{max} values from the J–V curve measured under standard reporting conditions.

(4) dV_{oc}/dT_c, dFF/dT_c, and dP_{max}/dT_c are compared with lab measurements, and J_{00i} and ΔE_i are corrected (total and spectral irradiance fixed). Table 1 compares published values of the maximum power temperature coefficients (in parts per thousand) with modelled values from this study.

(5) dV_{oc}/dI, dFF/dI, and dP_{max}/dI are compared with lab measurements and R_s, R_{sh}, and n_i are corrected (cell temperature and spectral irradiance fixed).

(6) The eight fitting parameters R_s, R_{sh}, n_i, and J_{00i} and ΔE_i are corrected, and steps (3) to (6) are repeated until the J–V characteristics are well reproduced by the modelling procedure. Table 2 summarizes the fitting parameters that were used in modelling P_{max}.

The computer code calculating P_{max} uses a numerical search routine. It does not apply other simplifying approximations to locate P_{max}. For the case of the two-terminal multijunction PV-device the J–V curve for each junction is computed first and then the multijunction J–V curve is constructed by summing the voltages at the same current.

2.2. Meteorological model and data

Within a three years effort one hundred thousand solar spectra were recorded in the wavelength range from 300 to 1100 nm [1]. These measured spectra were utilized to develop the semi-empirical model SEDES2 that calculates hemispherical solar spectral irradiance on a south tilted surface from three readily available meteorological data only: global and diffuse irradiance (alternatively direct irradiance), and dew point temperature (alternatively relative humidity and ambient temperature). Using atmospheric surface pressure instead of site elevation slightly

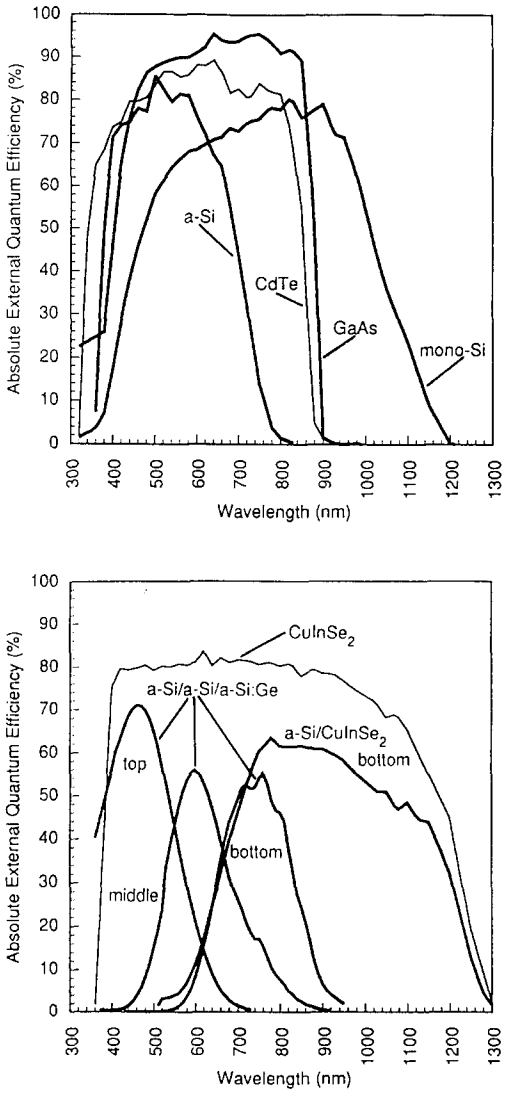

Fig. 1. Measured quantum efficiencies for production mono-Si, and state-of-the-art a-Si:H, CdTe and GaAs, a-Si:H/a-Si:H/a-SiGe:H three-junction tandem, $CuInSe_2$, and the bottom cell in a four-terminal tandem made of a-Si:H mechanically stacked on $CuInSe_2$.

improves calculations. Model output is hemispherical irradiance from 300 to 1400 nm with 10 nm resolution. Input and output are hourly data.

SEDES2 consists of the clear-sky approximation code "SPCTRAL2" [19], a normalization procedure and cloud cover modifiers derived from statistical analysis of the measured spectra as illustrated in fig. 2. There are four cloud cover modifiers for each wavelength corresponding to four zenith bins. These cloud

Table 1
Cell temperature dependence of P_{max} in parts per thousand and Kelvin at SRC ($dP_{max}/dT_c/P_{max}$):

Cell	Literature values (K^{-1})		Used in the model (K^{-1})
a-Si:H	−2.0 to −1.0	[15] (diff. alloys)	−2.1
	0	[16] (module meas.)	
CdTe	–	–	−4.3
a-Si:H/a-Si:H/ a-SiGe:H two-terminal	−2.2	[this work] (meas.)	−3.7
GaAs	−2.7	[15]	−2.0
	−1.5 to −2.8	[17]	
	−2.4	[18] (calculations)	
mono-Si	−3.5 to −3.2	[15]	−3.8
	−3.4 to −5.4	[17]	
	−3.3	[18] (calculations)	
$CuInSe_2$	−5.9	[15]	−5.2
	−2.4	[16] (module meas.)	
a-Si/$CuInSe_2$ four-terminal	–	–	−3.0

cover modifiers are slightly site dependent mainly because of particular site turbidity and surface albedo. Research to study site dependency is underway [20].

The solar cell operating temperature T_c of a module is mainly affected by the solar irradiance, but also by the ambient temperature and wind speed. Combined with the input data for the spectral model and solar geometry there are six parameters needed to predict the three quantities I, $E(\lambda)$, and T_c (see fig. 3).

The model applied to calculate the cell temperature T_c of a module was developed by Fuentes [21]. The required inputs include the plane-of-array irradiance, ambient temperature, wind speed, average array height above ground, anemometer height, and the "installed nominal operating cell temperature" (INOCT). INOCT is defined as the cell temperature of an installed array at NOCT conditions (800 W/m^2 insolation, 20°C ambient temperature, and 1 m/s wind speed). It differs from the NOCT temperature in that the mounting configuration is accounted for with INOCT. We utilize a fixed INOCT of 50°C for all modules. The model applied to calculate the plane-of-array irradiance I was developed by Perez et al. [22]. The required inputs include the global horizontal and diffuse (or direct beam) total irradiance.

Both codes, the Perez and the Fuentes model, are considered to be among the best currently available semi-empirical models which convert hourly averages of readily available meteorological data into parameters influencing PV-cell performance. Together with SEDES2 and the diode equation model this is the software package we utilized to predict the maximum power P_{max} and the hourly efficiency of seven different PV-technologies as illustrated in fig. 4. A similar software package has been developed by Heidler et al. [23].

The six meteorological inputs were taken from observations of the German meteorological network (DWD) at Stuttgart from 1987–1989. The input data were

Table 2
Main parameters of solar devices investigated

Cell	η_{SRC} (%)		E_g (eV)		Response > 5% (nm)	J_{sc} (A/m^2)	R_s (Ω m^2)	R_{sh} (Ω m^2)	J_{001} (A/m^2)	n_1 –	ΔE_1 (eV)	J_{002} (A/m^2)	n_2 –	ΔE_2 (eV)
a-Si:H		10.0		1.75	360– 790	156.2	8×10^{-4}	9.0	3×10^{7}	1.05	1.15	6×10^{10}	2.0	1.15
[CdS] CdTe		13.4		1.50	320– 880	245.1	5×10^{-4}	0.1	1.1×10^{13}	1.1	1.35	8×10^{11}	2.0	1.1
a-Si:H/			t:	1.75	360– 690	74.33	1.3×10^{-3}	0.9	1.7×10^{4}	1.0	1.02	5×10^{10}	2.0	1.15
a-Si:H			m:	1.75	460– 830	73.38	1.5×10^{-3}	1.0	6.9×10^{7}	1.1	1.15	6×10^{10}	2.0	1.15
a-SiGe:H			b:	1.35	590– 900	73.41	2×10^{-3}	0.8	6.5×10^{9}	1.1	1.37	2.5×10^{12}	2.1	1.0
(2 terminals)	all:	13.1			360– 900	–	–	–	–	–	–	–	–	–
[GaInP] GaAs		25.1		1.41	320– 900	278.1	1×10^{-4}	1×10^{4}	1×10^{10}	1.05	1.45	2×10^{14}	2.0	1.5
mono-Si		12.9		1.12	380–1180	270.6	2×10^{-4}	1×10^{3}	5×10^{10}	1.0	1.12	2×10^{10}	2.0	0.91
[ZnO/CdS]$CuInSe_2$		12.3		1.00	380–1280	355.6	2×10^{-4}	0.1	1.5×10^{11}	1.05	1.0	2×10^{12}	2.0	1.15
a-Si:H/	t:	10.0	t:	1.75	360– 790	156.2	8×10^{-4}	9.0	3×10^{7}	1.05	1.15	6×10^{10}	2.0	1.15
$CuInSe_2$	b:	6.1	b:	1.00	560–1280	170.8	2×10^{-4}	0.1	1.5×10^{11}	1.05	1.0	2×10^{12}	2.0	1.15
(4 terminals)	all:	16.1			360–1280	327.0	–	–	–	–	–	–	–	–

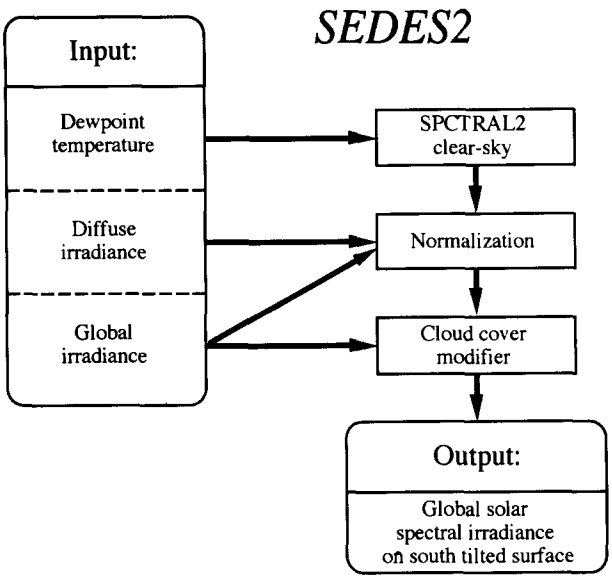

Fig. 2. The principal components of the semi-empirical spectral model SEDES2.

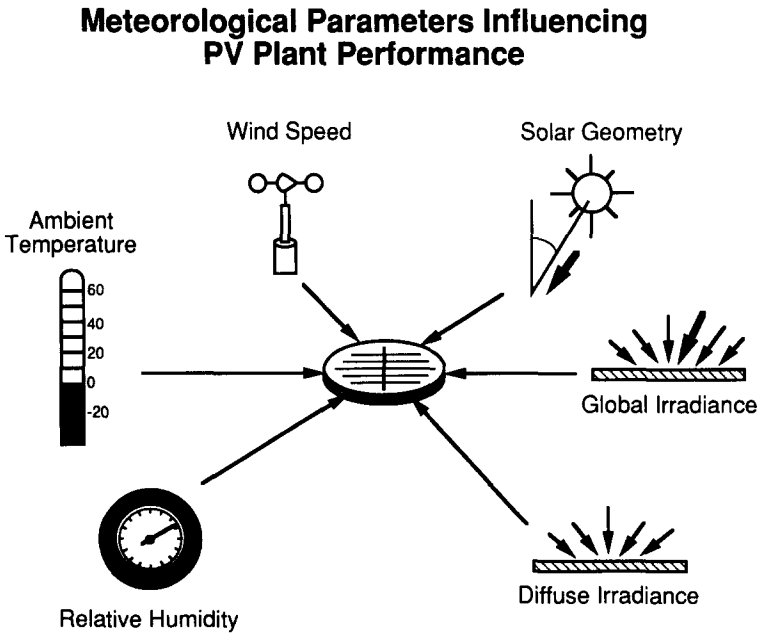

Fig. 3. The six parameters influencing PV-plant performance.

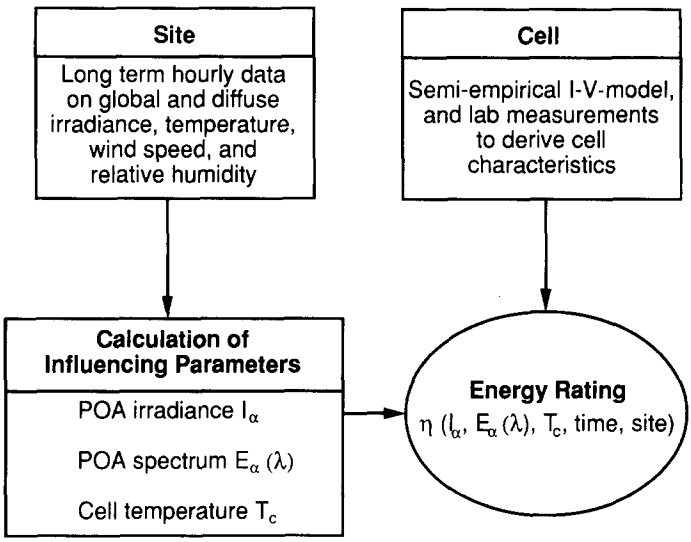

Fig. 4. The principal components of the semi-empirical software package used to compute the PV-power at hourly intervals over extended periods of time with measured site-specific meteorological data and technology dependent cell data.

checked with a comprehensive quality control procedure based on physical limits and consistency checks. If one of the elements did not pass, the hour was rejected. In addition, hours were taken into account only if global irradiance was above 40 W/m^2, angle of incidence on the latitude-tilted plane less than 85°, and zenith angle less than 82°. As a result of these restrictions, 30% of all daylight hours were selected out. Applying these limits avoids unreasonable results caused by extreme spectra which are irrelevant in terms of energy produced.

3. Spectral effects on efficiency

The literature which has been published about spectral effects on PV-device performance was reviewed by Riordan and Hulstrom [24,25]. The magnitude of spectral effects mainly depends on the band gap of the cells (a higher band gap leads to larger spectral effects), the time period of integration (longer integration periods reduce spectral effects), and the range of environmental conditions taken into account [26,27].

There were some suppositions that, because of the current mismatch in the multiple-cell devices under natural solar radiation conditions, spectral effects will cause multiple-cell devices to have no advantage over single-cell devices if they are series-connected [28]. Several studies, however, compared multiple-cell devices like $CuInSe_2$/a-Si:H [29,30], and a-Si:H/a-Si:H/a-SiGe:H [31,32] with the comparable single-cell devices and concluded that these multiple-cell devices outperform

the single-cell devices at least for clear-sky conditions. The spectral effects on the efficiency were greatest at low insolation where the contribution to the total energy delivered is small.

The parallel and independent configurations as an alternative are less sensitive to spectral fluctuations but require three- or four-terminal cells and, therefore, involve more complex processing for both forming the grids and mounting the cells in a module [33,34]. Another group of investigators studied spectral effects (temperature and irradiance) to optimize band gap and layer thickness for different devices (mainly III–V concentrator tandem cells) and different climates [17,35–39].

The American Society for Testing and Materials (ASTM), the International Electrotechnical Commission (IEC), and others have adopted particular spectral irradiance data sets as standard spectra. One of these is the "standard for solar spectral irradiance tables at air mass 1.5 for a 37° tilted surface" (ASTM standard E 892-87 or IEC standard 904). This spectrum was generated by the Solar Energy Research Institute (SERI) using the atmospheric transmittance model "BRITE" and the US standard atmosphere [40,41]. The US standard atmosphere contains 1.42 cm of precipitable water and 0.34 cm of ozone in a vertical column, and a rural aerosol model with sea level visibility of 25 km (aerosol optical depth of 0.27 at 500 nm). In our text we refer to it with "AM1.5 global".

To separate the effects of I, $E(\lambda)$, and T_c on efficiency η, we use a terminology similar to that introduced by Heidler et al. [23] and defined in table 3. The fraction $\eta_{E(\lambda)}/\eta_{SRC}$ describes the relative change in efficiency when a transition is made from standard reporting conditions (SRC) to conditions where $E(\lambda)$ becomes real, but the other two influencing parameters, T_c and I, are still fixed at their standard values. This ratio we call the spectral effect. Most solar cells are non-linear in T_c, I, and $E(\lambda)$. Therefore, on top of this "one-dimensional" spectral effect $\eta_{E(\lambda)}/\eta_{SRC}$ come those due to temperature $\eta_{E(\lambda)T_c}/\eta_{T_c}$ (a change in cell temperature influences the sensitivity to incident spectra variability) and due to the broadband insolation $\eta_{E(\lambda)I}/\eta_I$ (a decrease in insolation makes the device more sensitive to spectral variations if the efficiency is dependent on insolation especially for insolation conditions below 100 W/m^2). This point is made, because there is

Table 3
Definition of different efficiencies used in this investigation (the subscripts T_c, I or $E(\lambda)$ refer to the efficiency with that parameter "real")

	Total irradiance I	Cell temp. T_c	Spectral irradiance $E(\lambda)$
η_{SRC}	1000 W/m^2	25°C	AM1.5 global
η_{Tc}	1000 W/m^2	real	AM1.5 global
η_I	real	25°C	AM1.5 global
$\eta_{E(\lambda)}$	1000 W/m^2	25°C	real
$\eta_{E(\lambda)I}$	real	25°C	real
$\eta_{E(\lambda)Tc}$	1000 W/m^2	real	real
η_{RRC}	real	real	real

actually no clear definition of "spectral effects". The present investigation is confined on the one-dimensional spectral effect which would still remain if QE(λ) were not dependent on T_c and I.

3.1. Hourly spectral effects

Applying the software package presented above the hourly efficiency $\eta_{E(\lambda)}$ was calculated for the whole Stuttgart dataset by substituting $E(\lambda)$ in eq. (1) by

$$E(\lambda) \Rightarrow [E(\lambda)/I] \times 1000 \text{ W/m}^2. \tag{9}$$

The result is plotted in fig. 5 against I for all 9100 data points.

For insolation values above 800 W/m^2 there are, in general, no clouds, and the zenith angle is less than 60°. These conditions are close to the AM1.5 reference spectrum conditions. Therefore, the ratio $\eta_{E(\lambda)}/\eta_{SRC}$ in fig. 5 approaches one on the right hand side of the graphs. For insolation values below 200 W/m^2 overcast skies are predominant. Under this condition the relative spectral distribution is shifted towards shorter wavelengths [1]. As a result the efficiency of the devices increases. Extreme outliers above 1 are caused by clear skies and high angles of incidence when the cells mainly see the blue sky. This mainly happens in summertime, whereas the corresponding situation with low zenith angles but the red sun illuminating the arrays with low angles of incidence happens in wintertime and causes very low efficiencies. In between are situations with parly cloudy skies, high or low turbidity, high or low water vapor.

Table 4 shows the statistical mean of the ensembles of fig. 5 along with the standard deviation from the mean, maximum, and minimum ratios $\eta_{E(\lambda)}/\eta_{SRC}$ and the device response width (QE(λ) > 5%, according to table 2 and fig. 1). Supplementary to table 4, fig. 6 illustrates the distribution of the hourly spectral effect examplified with the a-Si cell.

As a general rule the distribution becomes narrower with increasing response width or decreasing band gap. This is even the case for the a-Si:H/a-Si:H/a-SiGe:H two-terminal device. As was pointed out by Smith and Wagner [31], Fain et al. [26], and Gorn et al. [42], mismatching the current of the component cells can increase the fill factor of the finished device (depending on the reverse characteristic of the cell). Therefore, the current mismatch losses are partly compensated for.

Fan's equation [33], which has often been applied for calculating the efficiency of series connected cells, is simply a weighted combination of the individual cells. This approach generally overestimates current mismatch losses. This is also the case for studies estimating the mismatch losses from short-circuit currents alone.

Figs. 5 and 6 along with table 4 give an idea on how important spectral effects are for the seven devices investigated. Spectral effects become an issue especially for higher band gap materials where the efficiency can change by more than 20% for hourly averages because of spectral variations (for our data set restricted to $I > 40$ W/m^2 and $z < 82°$). High band gap devices can gain 10% in efficiency under cloudy skies. For high ($I > 800$ W/m^2) insolation conditions, where the

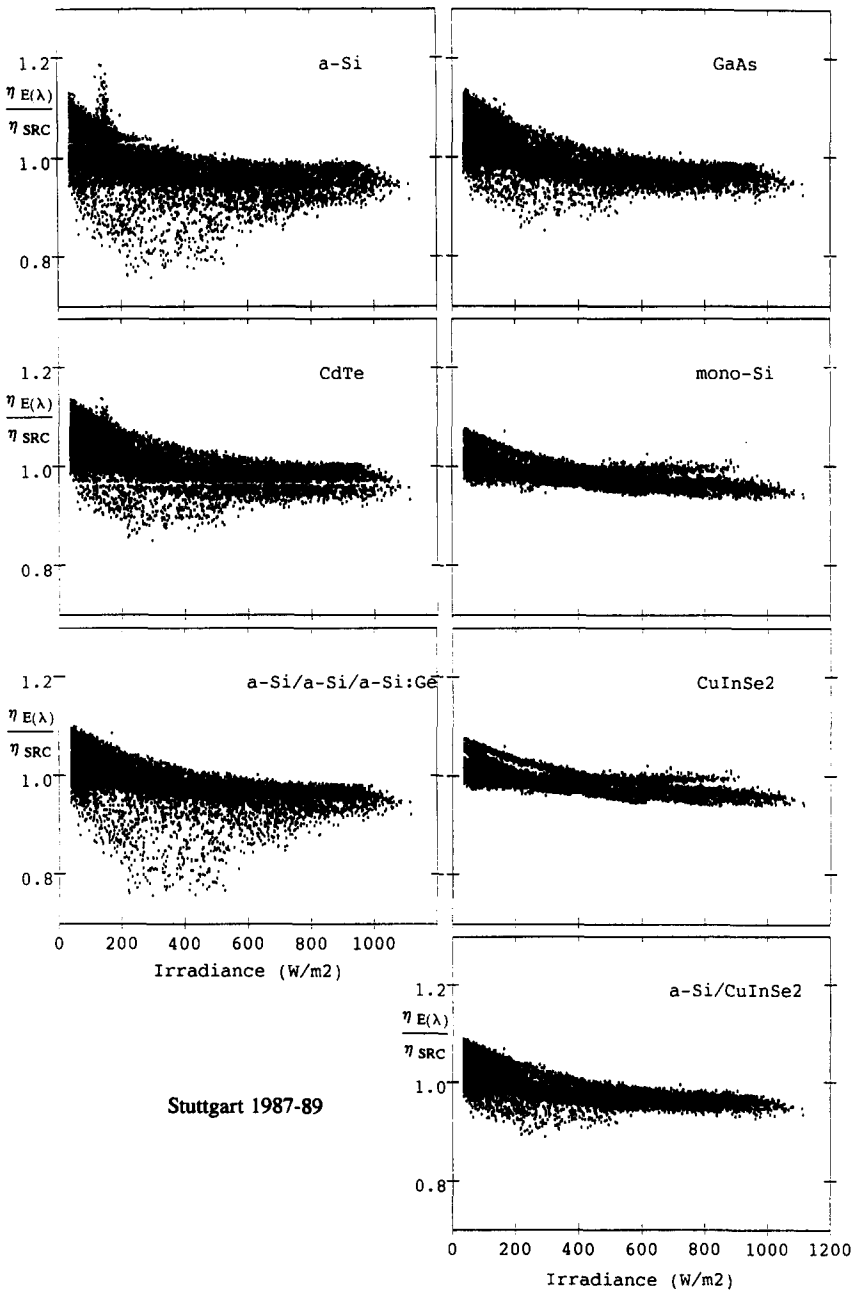

Fig. 5. Hourly spectral effect on efficiency.

Table 4
Mean, maximum, minimum, and standard deviation of all 9100 ratios $\eta_{E(\lambda)}/\eta_{SRC}$ in fig. 5

Device	Mean	Max.	Min.	Stand. dev.	Resp. width (nm)
a-Si:H	0.99	1.19	0.76	0.058	430
CdTe	1.01	1.14	0.85	0.048	560
a-Si:H/a-Si:H/ a-SiGe:H	0.99	1.10	0.76	0.048	540
GaAs	1.00	1.14	0.85	0.047	580
mono-Si	0.99	1.08	0.93	0.028	800
$CuInSe_2$	1.00	1.08	0.94	0.027	900
a-Si/$CuInSe_2$	0.99	1.09	0.89	0.035	920

major fraction of energy is produced, changes in η because of spectral variation are minimal even for series-connected multijunction devices.

3.2. Spectral effects on PV-system monitoring

Outdoor measurements of modules or systems are often compared with indoor data for the same modules or projected data for the systems after extrapolation to SRC. This enables the system engineer to detect possible alterations, losses, and failures within the system. While extrapolating outdoor measurements to SRC the correct determination of the cell temperature is very critical [4,43]. A calibrated reference cell spectrally matched to the modules under test can be used to minimize spectral effects.

If no reference is available, a frequently asked question is how large the error due to spectral effects is if one determines the efficiency of a PV system outdoors.

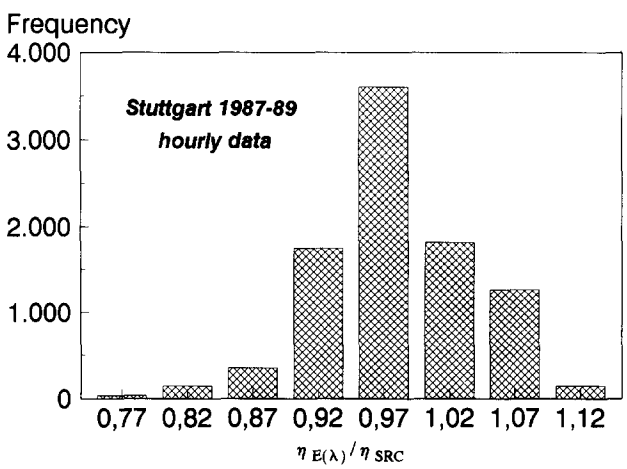

Fig. 6. Frequency distribution of the hourly spectral effect on efficiency.

Fig. 7 gives an answer for the Stuttgart site if one restricts all measurements to $z < 60°$. Under these conditions the maximum error for $I > 600$ W/m^2 becomes less than 10% for a-Si:H and 5% for mono-Si. Knaupp [44] confirmed these

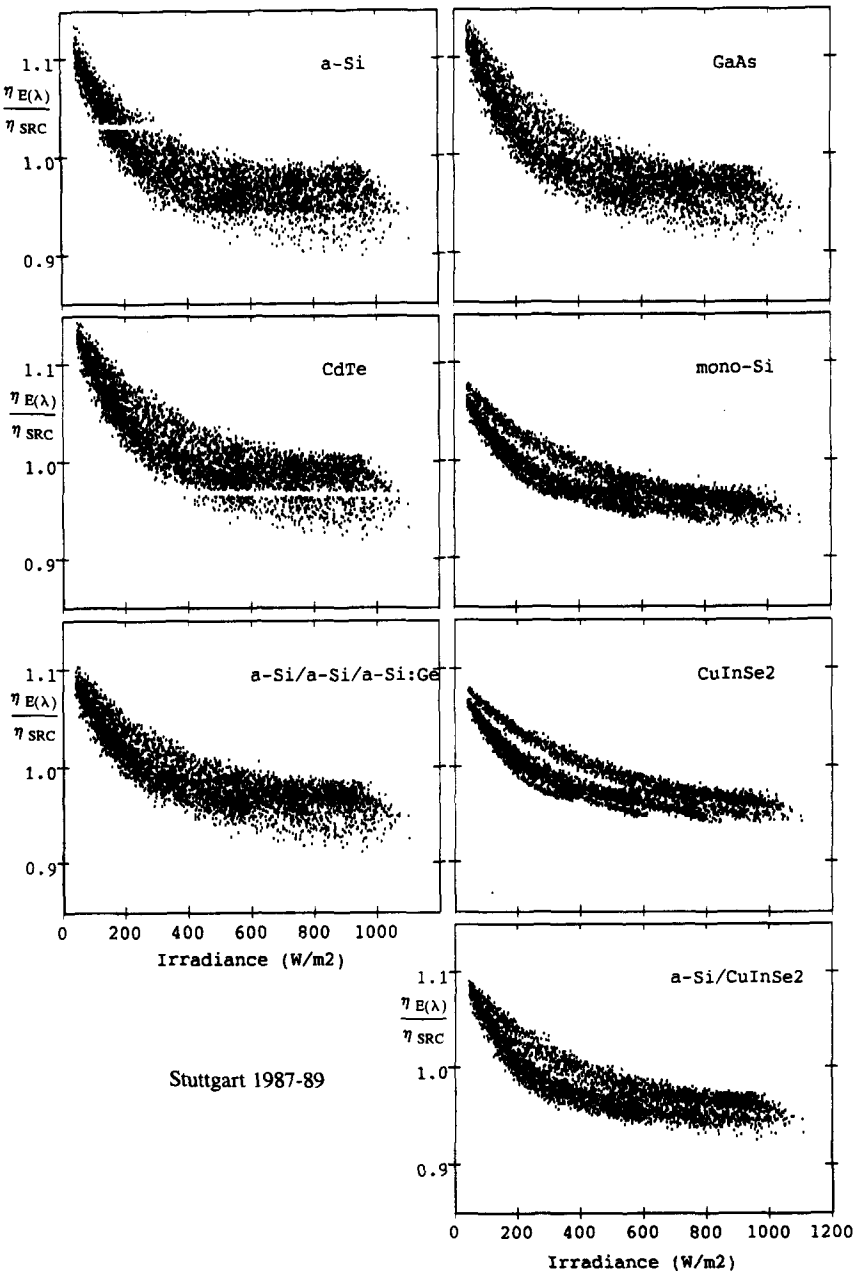

Fig. 7. Hourly spectral effect on efficiency for zenith angles less than 60°.

theoretically predicted numbers for mono-Si by measurements using a spectroradiometer. Very low efficiencies in fig. 7 are correlated with a low precipitable water vapor amount (lower than the 1.42 cm of the US standard atmosphere). During these conditions the spectrum is shifted to the infrared. Very high efficiencies in fig. 7 are correlated with cloudy skies where the spectrum is shifted to the blue.

3.3. Monthly and yearly spectral effects

Still fixing T_c and I at their standard value, monthly spectral effects were calculated from hourly $\eta_{E(\lambda)}$ by weighting with I according to

$$\eta_{E(\lambda),m} = \sum_m (\eta_{E(\lambda)} I) / \sum_m (I). \tag{10}$$

The monthly spectral effect is plotted in fig. 8 over the period of one year. There are pronounced differences between the specific monthly spectral effects on efficiency with increasing tendency for higher band gap devices. The biggest difference was calculated for amorphous silicon cells; their efficiency is 10% lower during winter.

Several outdoor experiments uncovered a 20% [45] or a 10% [46] drop in efficiency of amorphous silicon modules during winter. It was speculated that this effect is caused by higher temperatures in summer which anneal the amorphous silicon material and improve efficiency. Our results, however, show that the main reason for this drop in efficiency is the shift to the red in the spectrum during winter (see also Takigawa et al. [47]).

The yearly spectral effect also computed according to eq. (10) is comparably low for all devices. It ranges from -4% for a-Si:H to -2% for $CuInSe_2$.

Monthly and yearly spectral effects can be explained by looking at figs. 9 and 10 which show the yearly sum and the monthly sum for December of hemispherical solar spectral irradiance compared to the IEC-Standard. The calculations were performed with SEDES2 and the 1987–1989 Stuttgart data set. As can be seen, the standard matches the yearly spectrum very well. There are, however, particular months where this is not the case. Especially in wintertime high zenith angles shift the spectrum to the red, which causes a-Si:H cells to drop in efficiency, whereas the conditions are somewhat advantageous for mono-Si cells.

3.4. Comparison with temperature and total irradiance effects

Finally, the complete software package was used to put the monthly spectral effect on efficiency into perspective with the other two influences caused by variations in T_c and I. According to eq. (11) the monthly efficiency under prevailing conditions (real I, $E(\lambda)$, and T_c) was computed. Fig. 11 shows the monthly deviation from the efficiency under SRC for each month.

$$\eta_{RRC,m} = \sum_m (\eta_{RRC} I) / \sum_m (I), \tag{11}$$

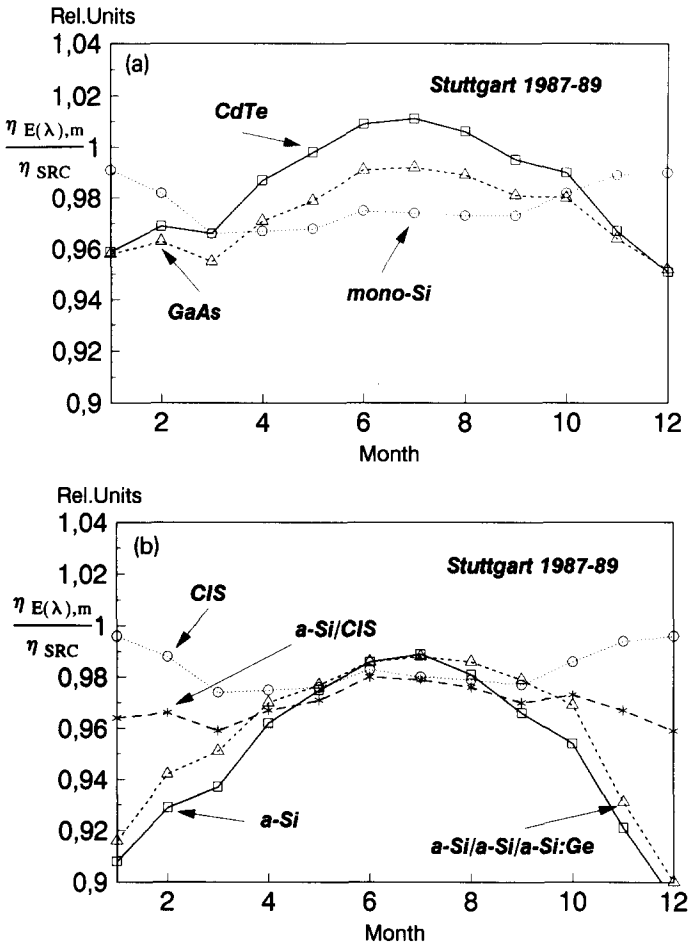

Fig. 8. Monthly spectral effect on efficiency (see eq. (10)).

The ratio $\eta_{\mathrm{RRC},m}/\eta_{\mathrm{SRC}}$ is lower than $\eta_{E(\lambda),m}/\eta_{\mathrm{SRC}}$ of fig. 8 during summer for all devices except the a-Si:H cell (because of its dependence on I). The difference between figs. 8 and 11 is mainly driven by the cell temperature dependence of $P_{\max}$ as given in table 1. As can be seen, T_c and $E(\lambda)$ effects partly compensate each other. One can conclude that for the high band gap devices a-Si, CdTe, and GaAs spectral effects are comparable to temperature effects during summer and clearly dominate monthly efficiencies during winter.

4. Critical operation periods

Because standardized terrestrial efficiency measurements are referenced to a fixed set of environmental conditions (SRC), they can only approximate the energy

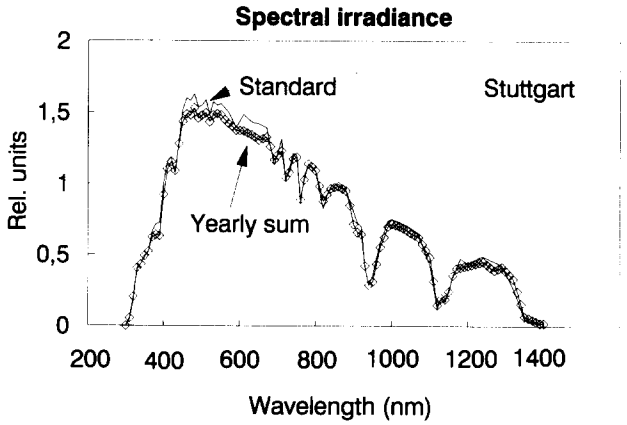

Fig. 9. Mean yearly sum of hemispherical solar spectral irradiance (latitude-tilted plane) and IEC-Standard, both normalized by their integral.

a specific device would deliver at a site where the temperature, and total and spectral irradiance differ from the reference conditions. Specifying performance at a given location or environment in terms of the average energy produced over a given time period is a desirable alternative to simply using the efficiency at SRC which is really an instantaneous value and is rarely duplicated in the field. At present, no standards exist for energy rating methods although several laboratories are working on the problem.

One possible approach is to apply outdoor measurement results to establish correlations between module power output and environmental parameters. The major predictor variables are global or plane-of-array irradiance, ambient tempera-

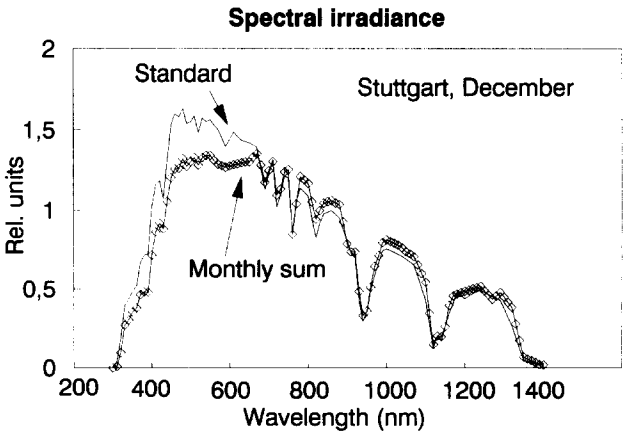

Fig. 10. Mean monthly sum of hemispherical solar spectral irradiance (latitude-tilted plane) and IEC-Standard, both normalized by their integral.

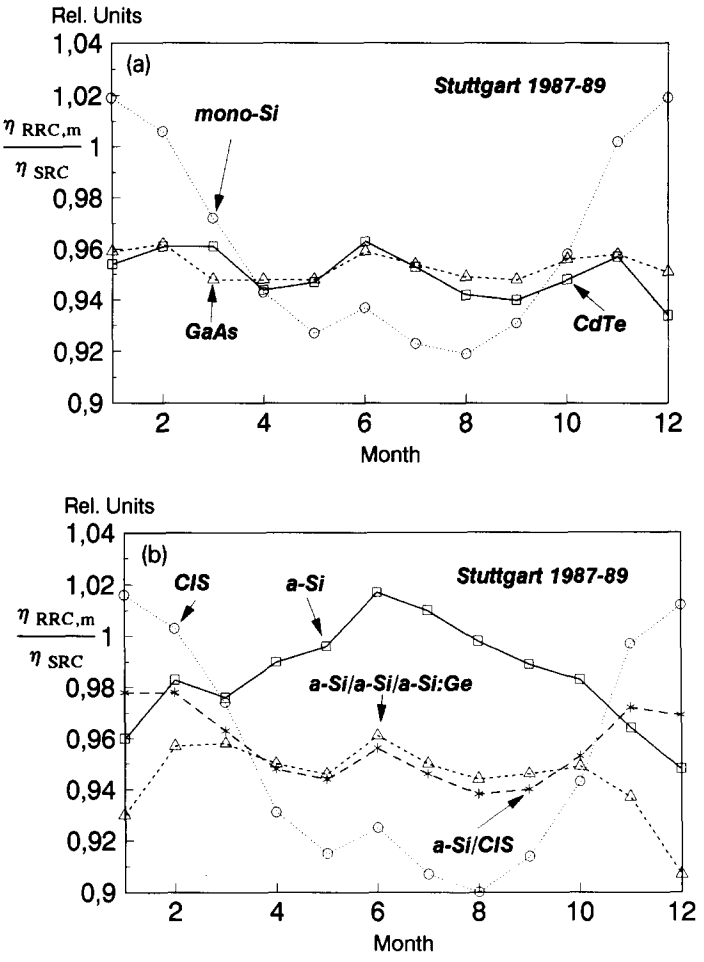

Fig. 11. Mean monthly efficiency under realistic reporting conditions normalized by the efficiency under standard reporting conditions (see eq. (11)).

ture, and sometimes wind speed. Multiple linear regression models can be applied to transfer a range of environmental conditions and periods to SRC [3,16,32,48–52] or to a "standard solar day" like the "AM/PM standard day". The AM/PM energy rating concept quantifies the energy output with respect to a standard temperature distribution (15–25°C), latitude (30°), and irradiance distribution (4.8 kWh/m^2 global horizontal versus time of the standard solar day) [29,53,54]. Major disadvantages of these methods are that spectral effects are not included, which makes these methods not applicable to higher band gap devices.

Our proposal (see also Heidler et al. [23]) is to apply the simulation technique illustrated in fig. 4 based on simulated time series specified by the six parameters of fig. 3. Depending on the specifications one can calculate the average site-specific energy output for a given system over a given time period.

Table 5
Mean efficiencies η^*_{COP} for critical operation periods normalized to η_{SRC} calculated according to eq. (12) for three years data from Stuttgart. Also given in parenthesis is the month (m) or hour (h) where the extreme values occur.

Condition	a-Si:H	CdTe	a-Si:H/a-Si:H/ a-SiGe:H 2-terminal	GaAs	mono-Si	$CuInSe_2$	a-Si:H/$CuInSe_2$ 4-terminal
Standard reporting Conditions η_{SRC}	10.0%	13.4%	13.1%	25.1%	12.9%	12.3%	16.1%
The whole year η^*_{annual}	0.99	0.95	0.95	0.95	0.95	0.94	0.95
Month with highest efficiency $\eta^*_{max(m)}$	1.02 (6)	0.96 (6)	0.96 (6)	0.96 (2)	1.02 (1)	1.02 (1)	0.98 (2)
Month with lowest efficiency $\eta^*_{min/(m)}$	0.95 (12)	0.93 (12)	0.91 (12)	0.95 (5)	0.92 (8)	0.90 (8)	0.94 (8)
Month with lowest irradiance $\eta^*_{lowI(m)}$	0.95 (12)	0.93 (12)	0.91 (12)	0.95 (12)	1.02 (12)	1.01 (12)	0.97 (12)
Hour with highest temperature $\eta^*_{highT(h)}$	0.95 (13)	0.88 (13)	0.88 (13)	0.93 (13)	0.85 (13)	0.81 (13)	0.89 (13)

Table 6
Critical operation periods for the most important PV-system configurations

PV-system configuration	Critical operation period
Grid-connected, fuel-saving mode, hydrogen production	The whole year
Peak demand supply	During peak demand (time of day, temperature)
Remote system for cooling	At high temperatures
Remote system with storage	During months with low irradiance
Pump system for agriculture	During growth time (time when water needed)

Using this approach, different rating methods were compared for each of the seven devices investigated. The five normalized mean efficiencies in table 5 result from an analysis of the most important PV-system configurations and the time period when their operation is most critical (see table 6). For a remote system the important factor is the output during the month with lowest irradiance. For the peak-load applications or remote systems for cooling, the temperature very often is the important parameter determining efficiency. For water pumping systems used in farming the months during the growing season are of interest. Correspondingly the mean efficiency η_{COP} during these critical operation periods (COP) was computed according to

$$\eta_{COP} = \sum_{COP} (\eta_{RRC} I) / \sum_{COP} (I), \tag{12}$$

and normalized to η_{SRC} which leads to η^*_{COP}.

From table 5 the following observations can be made:

(1) η^*_{annual}: The mean annual operating efficiency of the cells under the prevailing climate at Stuttgart is about 5% less than expected from SRC. The values η^*_{annual} show, however, that for grid-connected or hydrogen producing systems the current SRC do not bias the cells investigated.

(2) $\eta^*_{max(m)}$, $\eta^*_{min(m)}$: The spread between the month with the lowest and the highest efficiency is only 1% for GaAs, but 10% for mono-Si and 12% for $CuInSe_2$. The worst efficiencies occur in summer for the temperature-sensitive devices of our sample.

(3) $\eta^*_{lowI(m)}$: If the storage capacity of the system is designed with monthly irradiance profiles these numbers have to be considered very carefully. While mono-Si and $CuInSe_2$ perform very well this is totally different for the other devices of our sample.

(4) $\eta^*_{high(T(h))}$: It is obvious that the devices being less sensitive to cell temperature perform relatively better for periods with high ambient temperatures.

No general conclusions should be made about one technology versus another upon this study since the results are critically dependent on the modelled temperature and irradiance dependence, the state-of-the-art is rapidly improving, and cost versus performance figures have not been a part of this study. A statistically significant number of PV-devices must be accurately modelled for a variety of locations. The values of table 5, however, clearly demonstrate that the different

materials cause pronounced differences in response to the meteorological environment, which must be considered if one optimizes the economics and reliability of PV systems.

5. Conclusions

A software package was presented to simulate solar cell power production. It was applied for seven different solar cell technologies. The calculations were performed with meteorological input data from a cloudy site (Stuttgart, Germany), restricted to mean hourly irradiance levels above 40 W/m^2 and zenith angles less than 82°. Empirically derived solar cell parameters were presented for typical production mono-Si and state-of-the-art GaAs and thin-film technologies including CdTe, $CuInSe_2$, a-Si:H, and a-Si:H/a-Si:H/a-SiGe:H devices. This software package was utilized to investigate the effect variations in the solar spectral irradiance have on cell efficiency on a hourly, monthly and yearly time scale. It was also studied how the other two environmental parameters, total irradiance and cell temperature, influence the performance of the different devices.

Compared to approaches relying on outdoor measurements the software package presented here has some advantages:

(1) The performance of devices which have not yet been realized as modules (or cells) can be investigated and forecasted.

(2) Each run of the software is cheap compared to the costs of long-term measurements.

(3) The influencing parameters can be investigated independently.

(4) Spectral effects can be included more easily.

Compared to earlier computer studies the present one includes spectra under cloudy skies and real sets of meteorological data where all elements were measured at the same time. Real quantum efficiencies and the non-ideal behaviour of solar cells are taken into account.

From an investigation of the most important PV-system technologies critical operation periods can be identified. Five efficiency values averaged over different time periods are sufficient to determine the solar cell efficiency for the critical operation periods. For the seven particular cells the five efficiencies were calculated and compared with their efficiency under standard reporting conditions (SRC). The performance of the investigated devices relative to their performance under SRC shows pronounced differences for the critical operation periods, which clearly demonstrates the need for a new energy rating scheme taking into account the site-specific meteorological environment.

The PV-community is in state of flux concerning rating methods that are different from SRC which are 25°C cell temperature, 1000 W/m^2 total irradiance, and the ASTM E 892 or IEC 904 global reference spectrum. For any new rating method to be widely accepted, the support of the relevant standard organization and PV-manufacturers is required. Before any specific recommendation on module rating methods can be made, the following points should be considered:

Uses

(1) Better comparison of module technologies and vendors should be possible by a new rating scheme.

(2) The new rating scheme will be used for (see also Firor et al. [55]) pricing, designing, sizing, acceptance testing, warranty discussions, regulatory justification, comparison of initial and long-term operating parameters to identify system degradation mechanisms and system problems, forecast of plant output, and determining capacity for qualifying facility's capacity credit.

(3) A meaningful rating scheme sets production goals for the PV-manufacturers. Furthermore, it encourages them to offer application- and site-specific products.

(4) An energy rating scheme gives incentives to optimize energy instead of power.

Criteria

(1) Rating methods should be developed from a customer/user/system designer perspective.

(2) There should be no technology or application bias.

(3) One simple, fast and accurate rating like η_{SRC} will always be needed for research and high volume production measurements.

Open questions

(1) Should a single rating method be adopted or should a variety of ratings be adopted for different applications?

(2) Should the rating(s) be performed at the maximum power point only or should the rating(s) be performed as a function of voltage? This is important because many power trackers or inverters operate at a fixed voltage and must be properly sized for the specific PV-technology.

(3) Should the rating be based upon power and/or energy?

(4) Should the rating be site-specific?

(5) If a power rating is used, should a single reference spectrum be used or a distribution of spectra over time of day, location, time of year be applied?

(6) Should a module rating be developed independently from system rating? This is important because the module itself is not independent of the system. Mismatch and load depend on the system and the module temperature depends on the module position within the array/system and the type of mounting.

(7) Should the reflection losses on the module surface be taken into account?

The present investigation has not been able to address all these questions. Some conclusions can be drawn:

(1) Five meteorological parameters (global and diffuse irradiance, ambient temperature, wind speed, relative humidity, and solar geometry) are sufficient to determine the meteorological environment in which a PV-system operates.

(2) For the new technologies with high band gaps spectral effects influence the efficiency as much as cell temperature.

(3) Spectral effects do no cause amorphous silicon multijunction two-terminal devices to be outperformed by single-junction structures not even for cloudy skies.

(4) It is possible to estimate the spectral error from fig. 7 if one has to perform an outdoor PV-system efficiency measurement.

(5) The main reason for the drop in efficiency of amorphous silicon modules during winter is the shift to the red in the spectrum.

(6) The IEC 904 global reference spectrum matches the yearly spectrum at Stuttgart very well, but for particular months there are pronounced differences between the monthly spectra and the standard.

(7) If the market will be shared by devices having different responses to the five parameters, the numbers from table 5 clearly demonstrate the need for energy rating schemes supporting system designers to pick the appropriate technology for their specific application and site-specific climate.

(8) From an investigation of the most important PV-system technologies critical operation conditions can be identified. Five efficiency values averaged over different time periods are sufficient to determine the solar cell efficiency for the critical operation conditions.

New methods have to be developed to address the open question in detail. Both, simulation techniques and long-term outdoor experiments are appropriate. To improve a simulation approach based on a software package like in fig. 4 the following research areas should be intensified:

(1) Resource assessment: It is still a problem to obtain reliable data on the solar resource for all the interesting sites.

(2) Spectral modelling: SEDES2 and other spectral models have to be verified and improved with data from different climates.

(3) Module temperature modelling: It should be possible to predict the cell temperature for different module technologies and sites more precisely with improved models.

(4) Solar cell modelling: The superposition principle is inappropriate for thin film devices.

(5) Solar cell data: More data are needed for the cell response as a function of total irradiance and cell temperature.

(6) System Modelling: For the time being, the "system" in our simulations includes the cell only. A more comprehensive software package has to consider other losses as discussed in the introduction. It would include simulation models which have been developed for module, array and power control unit losses as well as storage and back-up performance.

Both research centers, the National Renewable Energy Laboratory (NREL) and the Centre for Solar Energy and Hydrogen Research (ZSW) cover these six areas with their common research in order to develop a better rating scheme for PV-cells, arrays, and systems. Right now, no specific recommendation about what rating scheme should be adopted can be given. A more comprehensive modelling study has to be performed first, in which all the different rating methods (like SRC, NOCT, AM/PM, and the five parameters proposed here) will be compared for a variety of PV-technologies. A software package like the one presented here allows the performance of various PV-technologies to be directly compared and forecasted under identical "real-world" conditions. This complex approach could

result in improved power and energy rating schemes having a relatively simple structure.

Acknowledgements

We would like to thank A. Bakenfelder, Dr. G. Bauer, Dr. U. Eicker, Dr. C. Riordan, and Dr. W. Spirkel for their comments on the manuscript. This work was supported by the German Ministry of Research and Technology under contract number 0329047A and the US Department of Energy under contract number DE-AC02-83CH10093.

Nomenclature

AM	air mass
c	speed of light (2.997925×10^8 m/s)
CIS	$CuInSe_2$
COP	critical operation period
E_g	energy gap (eV)
$E(\lambda)$	hemispherical spectral irradiance on tilted plane ($W/m^2/nm$)
FF	fill factor
h	hour
h	Planck's constant (6.6262×10^{-34} J s)
I	total irradiance on tilted plane (W/m^2)
INOCT	installed nominal operating cell temperature (°C)
J_{dark}	dark current density (A/m^2)
J_{0i}	reverse saturation current density (A/m^2)
J_{00i}	pre-exponential factor in Meyer–Neldel rule (A/m^2)
J_{out}	output current density (A/m^2)
J_{ph}	light generated current density (A/m^2)
J_{sc}	short-circuit current density (A/m^2)
k	Boltzmann's constant (8.617×10^{-5} eV/K)
m	month
n_i	diode quality factor
NOCT	nominal operating cell temperature (°C)
P	output power (W/m^2)
P_{max}	maximum output power (W/m^2)
POA	plane-of-array
q	electron charge (1.60219×10^{-19} A s)
QE(λ)	external quantum efficiency
RRC	realistic reporting conditions
R_s	series resistance (Ω m^2)
R_{sh}	shunt resistance (Ω m^2)
SRC	standard reporting conditions

T_c	cell temperature (°C)
V	voltage across diode (V)
V_{oc}	open-circuit voltage (V)
V_{out}	output voltage (V)
z	zenith angle
α	tilt angle
ΔE_i	activation energy for J_{0i} (eV)
λ	wavelength (nm)
η	efficiency
η^*	η_{COP} normalized to η_{SRC}

References

[1] S. Nann and S. Riordan, J. Appl. Meteorol. 30 (1991) 447.
[2] K.A. Emery and C.R. Osterwald, Curr. Top. Photov. 3 (1988) 302.
[3] C. Jennings, Outdoor versus rated photovoltaic module performance, in: Proc. 19th IEEE PV Specialists Conf., New Orleans, 1987.
[4] W. Knaupp, Performance of PV-modules at ZSW, in: Proc. 5th Int. PV Science and Engineering Conf., Kyoto, 1990.
[5] W.H. Bloss, H.P. Hertlein, W. Knaupp, S. Nann and F. Pfisterer, in: Solar Power Plants: Photovoltaic Power Stations, Eds. C.J. Winter, R.L. Sizmann and L.L. Vant-Hull (Springer, New York, 1991).
[6] S. Nann, Sol. Energy 45 (1990) 385.
[7] T.J. Coutts and N.M. Pearsall, Appl. Phys. Lett. 44 (1984) 134.
[8] C. Goradia and V.G. Weizer, Appl. Phys. Lett. 45 (1984) 1298.
[9] J. Beier and K. Bücher, Comparison of dark and light I-V curves of solar cells, in: Proc. 10th EC PV-Conference, Lisbon, 1991.
[10] M.S. Bennett and R.R. Arga, Sol. Cells 18 (1986) 289.
[11] J.R. Sites and P.H. Mauk, Sol. Cells 27 (1989) 411.
[12] J.R. Sites, H. Tavalkolian and R.A. Sasala, Sol. Cells 29 (1990) 39.
[13] J. Bruns, S. Gall and H.G. Wagemann, Simulation and analysis of the bias dependent spectral response of a-Si:H pin solar cells, in: Proc. 9th EC PV Solar Energy Conf., Freiburg, 1991.
[14] J. Burdick and T. Glatfelter, Sol. Cells 18 (1986) 301.
[15] C.R. Osterwald, Comparison of the temperature coefficients of the basic I-V parameters for various types of solar cells, in: Proc. 19th IEEE PV Specialists Conf., New Orleans, 1987, p. 188.
[16] W.R. Bottenberg and D. Reinker, Outdoor performance of hybrid, four-terminal tandem photovoltaic modules based on thin film silicon: hydrogen and copper indium diselenide, in: Proc. 20th IEEE PV Specialist Conf., Las Vegas, 1988, p. 1230.
[17] M.W. Wanlass, K. Emery, T. Gessert, G. Horner, C. Osterwald and T. Coutts, Sol. Cells 27 (1989) 191.
[18] J.C.C. Fan, Sol. Cells 17 (1986) 309.
[19] R.E. Bird and C. Riordan, J. Climate Appl. Meteor. 25 (1986) 87.
[20] S. Nann, A. Bakenfelder, C. Riordan and R. Schelp, Solar spectral irradiance under clear and cloudy skies: Testing a model at different sites, in: Proc. ISES Solar World Cong., Denver, 1991.
[21] M. Fuentes, in: A simplified thermal model for flat-plate photovoltaic arrays, Sandia Report 85-0330 (Sandia Nat. Lab., Albuquerque, NM, 1987).
[22] R. Perez et al., Sol. Energy 44 (1990) 271.

[23] K. Heidler, A. Raicu and H.R. Wilson, A new approach for the performance evaluation of solar cells under realistic reporting conditions, in: Proc. 21st IEEE PV Specialist Conf., Kissimmee, 1990.
[24] C. Riordan and R. Hulstrom, in: Summary of studies that examine the effects of spectral solar radiation variations on PV device and design performance, SERI Report 215-3437 (Solar Energy Research Institute, Golden, CO, 1989).
[25] C. Riordan and R. Hulstrom, Curr. Top. Photo. 4 (1990).
[26] P. Fain, S.R, Kurtz, C. Riordan and J.M. Olson, Sol. Cells 31 (1991) 259.
[27] H.R. Wilson and M. Hennies, Sol. Energy 42 (1989) 273.
[28] I. Chambouleyron and F. Alvarez, Conversion efficiency of multiple-gap solar cells under different irradiance conditions, in: Proc. 18th IEEE PV Specialist Conf., Las Vegas, 1985, p. 533.
[29] K. Mitchell, R. Rifai and L. Fabick, Performance modeling of thin film tandem PV-modules, in: Proc. 19th IEEE PV Specialists Conf., New Orleans, 1987.
[30] M. Andersson, L. Stolt, E. Wallinder and L. Dahlgreen, The effect of solar spectrum variations on the efficiency of tandem solar cells in a Swedish climate, in: Proc. 8th EC PV Conf., Florence, 1988.
[31] Z.E. Smith and S. Wagner, Spectral dependence of performance in multijunction amorphous silicon solar cells, in: Proc. 19th IEEE PV Specialists Conf., New Orleans, 1987, p. 204.
[32] J. Burdick and T. Glatfelter, Outdoor performance studies of a-Si alloy multijunction solar cells using simulated solar illumination, in: Proc. 21st IEEE PV Specialists Conf., Kissimmee, 1990.
[33] J.C.C. Fan and B.J. Palm, Sol. Cells 10 (1983) 81.
[34] J.M. Gee, Sol. Cells 24 (1988) 167.
[35] J.C.C. Fan, B.Y. Tsaur and B.J. Palm, Optimal design of high-efficiency tandem cells, in: Proc. 16th IEEE PV Specialists Conf., San Diego, 1982, p. 692.
[36] D.L. King and R.B. Siegel, Solar spectrum influence on the annual performance of AlGaAs/Si stacked cells, in: Proc. 17th IEEE PV Specialists Conf., Kissimmee, 1984, p. 944.
[37] M.E. Nell and A.M. Barnett, The spectral p-n junction model for tandem solar cell design, in: Proc. 19th IEEE PV Specialists Conf., New Orleans, 1987, p. 257.
[38] S. Kurtz, P. Faine and J.M. Olson, J. Appl. Phys. 68 (1990) 1890.
[39] S. Kurtz, J.M. Olson and P. Faine, Sol. Cells 30 (1991) 501.
[40] R.L. Hulstrom, R. Bird and C. Riordan, Sol. Cells 15 (1985) 365.
[41] C. Riordan and R. Hulstrom, What is an air mass 1.5 spectrum, in: Proc. 21st IEEE PV Specialists Conf., Kissimmee, 1990.
[42] M. Gorn, C. Curran, A. Antoine-Labouret and J.P.M. Schmitt, Investigation of spectral mismatch in a-SiGe:H based tandem solar cells by optical modelling, in: Proc. 10th EC PV Conf., Lisbon, 1991.
[43] G. Blaesser and E. Rossi, Sol. Cells 25 (1988) 91.
[44] W. Knaupp, Power rating of photovoltaic modules from outdoor measurements, in: Proc. 22nd IEEE PV Spec. Conf., Las Vegas (1991).
[45] PVUSA Project Team, PVUSA progress report, PVUSA, Davis, 1991.
[46] P. Ragot et al., Analysis of performance of amorphous silicon modules by experimentation in indoor and outdoor conditions, in: Proc. 10th EC PV Sol. Energy Conf., Lisbon, 1991.
[47] K. Takigawa, H. Kobayaski, Y. Takeda, A field evaluation of power efficiency degradation on amorphous PV modules, in: Proc. 4th Int. PV Science and Engineering Conf., Sydney, 1989.
[48] R.W. Taylor, Sol. Cells 18 (1986) 335.
[49] L.B. Fabick, R. Rifai, K. Mitchell, T. Woolston and J. Canale, Outdoor module testing and comparison of photovoltaic technologies, in: Proc. 19th IEEE PV Specialists Conf., New Orleans, 1987, p. 182.
[50] T. Glatfelter and J. Burdick, A method for determining the conversion efficiency of multiple-cell photovoltaic devices, in: Proc. 19th IEEE PV Specialists Conf., New Orleans, 1987, p. 1187.
[51] E. Gianoli-Rossi and K. Krebs, Energy rating of PV modules by outdoor response analysis, in: Proc. 8th EC PV Solar Energy Conf., Florence, 1988.
[52] B. Marion and G. Atmaram, Seasonal performance of three PV technologies, in: Proc. 21st IEEE PV Specialists Conf., Kissimmee, 1990.

[53] C.F. Gay, J.E. Rumburg and J.H. Wilson, "AM/PM"-All-day module performance measurements, in: Proc. 16th IEEE PV Specialists Conf., San Diego, 1982, p. 1041.
[54] J.P. Rumburg, Energy-based module ratings compared with field performance of single crystal, polycrystalline, and ribbon silicon photovoltaic modules, in: Proc. 17th IEEE PV Specialists Conf., Kissimmee, 1984.
[55] K. Firor, C.M. Whitaker and C. Jennings, Utility use of PV system ratings, in: Proc. 21st IEEE PV Specialists, Conf., Kissimmee, 1990.